Brain Functional Networks Based on Resting-State EEG Data for Major Depressive Disorder Analysis and Classification

Bingtao Zhang, Guanghui Yan, Zhifei Yang, Yun Su, Jinfeng Wang, and Tao Lei, *Senior Member, IEEE*

***Abstract*— If the brain is regarded as a system, it will be one of the most complex systems in the universe. Traditional analysis and classification methods of major depressive disorder (MDD) based on electroencephalography (EEG) feature-levels often regard electrode as isolated node and ignore the correlation between them, so it's difficult to find alters of abnormal topological architecture in brain. To solve this problem, we propose a brain functional network framework for MDD of analysis and classification based on resting state EEG. The phase lag index (PLI) was calculated based on the 64-channel resting state EEG to construct the function connection matrix to reduce and avoid the volume conductor effect. Then binarization of brain function network based on small world index was realized. Statistical analyses were performed on different EEG frequency band and different brain regions. The results showed that significant alterations of brain synchronization occurred in frontal, temporal, parietal-occipital regions of left brain and temporal region of right brain. And average shortest path length and clustering coefficient in left central region of theta band and node betweenness centrality in right parietal-occipital region were significantly correlated with PHQ-9 score of MDD, which indicates these three network metrics may be served as potential biomarkers to effectively distinguish MDD from controls and the highest classification accuracy can reach 93.31%. Our findings also point out that the brain function network of MDD patients shows a random trend, and small world characteristics appears to weaken.**

***Index Terms*— Major depressive disorder, electroencephalography, brain functional networks, phase lag index, abnormal topological architecture.**

I. Introduction

NOWADAYS major depressive disorder (MDD) has quietly become the second largest disease in the worldwide [1], and its typical symptoms include slow thinking, persistent low mood, anhedonia, and cognition impairment of brain function [2]. According to data disclosed by the World Health Organization (WHO), there are more than 350 million people suffering from MDD and the growth rate of patients in the past decade is about 18% [3]. It is estimated that about 850,000 suicides caused by MDD each year [4], accounting for 53.7% of all suicides [5]. With the high morbidity and mortality of MDD, it is critical to understand the underlying neurophysiological and brain function basis of MDD for the effective prevention and treatment of this mental illness.

Within the past few decades, considerable investigations on MDD have been continuously explored and advanced from the perspective of structure and function in brain using morphological or neurobiological features. These investigations, based on various physiological techniques such as functional magnetic resonance imaging (fMRI), magnetoencephalogram (MEG) and EEG, have been widely used to assess difference of MDD compared with controls. Combined with fMRI and morphological feature volume, Yao *et al.* [6] found that the atrophy region of amygdala and hippocampus has a slight tendency of expanding to other sub-regions with the progression of MDD. Based on the spontaneous oscillating neuromagnetic activity of MEG, the study found that the correlation between age and neurobiological feature Lempel-Ziv complexity disappeared in MDD patients [7]. Taking physiology and behavior as the breakthrough point, the study by [4] integrates pervasive EEG

Manuscript received August 19, 2020; revised November 15, 2020 and December 1, 2020; accepted December 6, 2020. Date of publication December 9, 2020; date of current version March 1, 2021. This work was supported in part by the National Natural Science Foundation of China under Grant 61962034, Grant 61941109, and Grant 61862058, in part by the Tianyou Youth Talent Lift Program of Lanzhou Jiaotong Univesity, in part by the Opening Foundation of the Key Laboratory of Opto-Technology and Intelligent Control, Lanzhou Jiaotong University, Ministry of Education, under Grant KFKT2020-13, and in part by the Scientific Research Innovation Project of School of Electronics and Information Engineering, Lanzhou Jiaotong University. *(Corresponding author: Bingtao Zhang.)*

Bingtao Zhang is with the School of Electronic and Information Engineering, Lanzhou Jiaotong University, Lanzhou 730070, China, also with the Key Laboratory of Opto-Technology and Intelligent Control, Ministry of Education, Lanzhou Jiaotong University, Lanzhou 730070, China, and also with the School of Information Science and Engineering, Lanzhou University, Lanzhou 730000, China (e-mail: zhangbingtao321@163.com).

Guanghui Yan and Zhifei Yang are with the School of Electronic and Information Engineering, Lanzhou Jiaotong University, Lanzhou 730070, China.

Yun Su is with the College of Computer Science and Engineering, Northwest Normal University, Lanzhou 730070, China, and also with the School of Information Science and Engineering, Lanzhou University, Lanzhou 730000, China.

Jinfeng Wang is with the Sleep Medicine Center of Gansu Province, Gansu Provincial People's Hospital, Lanzhou 730000, China.

Tao Lei is with the School of Electronic Information and Artificial Intelligence, Shaanxi University of Science and Technology, Xi'an 710021, China.

Digital Object Identifier 10.1109/TNSRE.2020.3043426

features and sound features into multi-agent strategy to realize convenient MDD detection.

However, human brain is a complex system consisting of about 10^{11} neurons and about 10^{15} synapses connecting these neurons. It is difficult to reveal the pathophysiological mechanism alterations of MDD hidden in the human brain only from the perspective of morphological or neurobiological features. In recent years, with the development of complex network theory based on graph theory [8], many researchers have demonstrated that brain networks can be constructed by fMRI, MEG and EEG data and resultant brain networks show many important topological properties [9]. Moreover, many accumulating evidences show that neuropsychiatric disorders were closely associated with abnormal topological alterations of brain networks [10]. Yu *et al*. pointed out that functional connectivity is an effective method to investigate brain abnormalities of Alzheimer's disease (AD), and provides a potential tool for identifying neurological diseases from the perspective of functional networks with EEG signals, especially for the identification of AD [11]. These studies provide a new avenue to understand the pathological mechanism of MDD.

From the above, this article intends to study the topological structure alterations of MDD from the level of brain function network connection, and then explore its pathophysiological mechanism and potential biomarkers. It is well known that fMRI has high spatial resolution, while MEG and EEG have high temporal resolution [12]. Brain functional connectivity is defined as mechanism for the coordination of temporal dependence activity between different neural assemblies of spatially separate [13]. Hence, EEG and MEG provide a satisfactory resolution to approach the temporal evolution of functional connectivity process related to brain activity from health into disease, compared with fMRI. EEG is widely used by scientists to study brain functions and to diagnose neurological diseases, abnormal of EEG signal is generally manifested as alterations in the signal pattern of the subject [14]. Meanwhile, considering EEG has the advantages of high time resolution, non-invasive, safe, easy operation and low cost [15]. It is more suitable for constructing brain function networks, so this study pays more attention to analysis and classification of EEG-based brain function for MDD.

Traditional method of the detection MDD or depression based on EEG feature-level has its inherent advantages. For example, feature-level fusion technology was used to construct multimodal model by fusing different EEG data sources for detection depression patients from normal controls, and the highest classification accuracy of 86.98% was obtained [2]. Its main advantage of this method is that EEG data obtained by fusing different audio stimuli to improve the classification accuracy. Zhang *et al.* proposed a multi-agent based fusion strategy of EEG features and voice features to achieve depression detection, and the classification accuracy 86.64% was achieved [4]. The main advantage of this method is that it integrates the universal EEG features and paralinguistic behaviors features to improve the classification accuracy. Despite the traditional method has its advantages and achieves EEG fusion in the feature-level, it often regard electrode as isolated node and ignore the correlation between electrodes, so it's difficult to find changes of abnormal topology in brain caused by MDD.

According to previous researches, we found that there are two critical issues need to be resolved in the construction process of brain functional network. First, which state of EEG data is most suitable for the construction of brain function network? Second, which coupling method is most suitable for the construction of real cortical brain networks? Both require further investigation and determination. To avoid interference from other physiological electrical signals such as EOG and EMG, etc., during the EEG recording process, it is necessary for the subjects to maintain a state of quiet, relaxation, awake and closed eyes in this process. The resting state just meets these needs. Moreover, many studies have confirmed that resting state EEG can be effectively used for the construction of brain function networks. In [16] resting state EEG was used to investigate the alterations of brain network metrics of the minimum spanning tree in dyslexia readers. By analyzing the resting state EEG data of schizophrenia patients, exploring the alterations in the temporal and spatial of their brain structure [17]. Research on brain function network based on resting state EEG, it is found that acupuncture can modulate the activity of human brain, and different acupuncture operations have different effects on brain functional network [18]. Siuly *et al.* developed a new framework for automatic detection of patients with mild cognitive impairment (MCI) using resting state EEG data [19]. Another problem is typical coupling calculation methods of functional connectivity matrix include correlation and coherence [20]. However, these methods are susceptible by the strong influence of volume conduction. To address this problem, the researchers suggest that functional connectivity should be analyzed according to source space rather than sensor space. Meanwhile, reducing and avoiding the influence of volume conduction on the construction of real cortical brain network [21], [22], the robust volume conduction method of PLI just meets these needs. Many previous studies have confirmed the feasibility of this idea. PLI has been applied to analyze the brain function network of patients with Alzheimer disease, dyslexics and so on [23]–[25]. In [26] PLI was also utilized to investigate the influence of acupuncture on the phase synchronization of EEG in different brain regions. In addition, some previous studies have applied PLI to depression [27]–[29].

How to effectively analyze the brain function networks and classification MDD after it is constructed. We have done a lot of literature investigation. In aspect of brain function networks analysis, a novel frequency analysis method was designed and used to reveal imaging marker for adolescent generalized anxiety disorder [30]. Based on the brain area analysis strategy, relative power and coherence of EEG series in patients with mild cognitive impairment (MCI) with diabetes were studied [31]. Yu *et al*. used graph theory to analyze the brain functional network, and revealed that brain functional connectivity undergoes obvious alter under different conditions: pre-acupuncture, acupuncture, and post-acupuncture [32]. Recently, an article published in Nature Neuroscience: analyzing several problems of intergroup conflicts using inter-brain synchronization mechanisms,

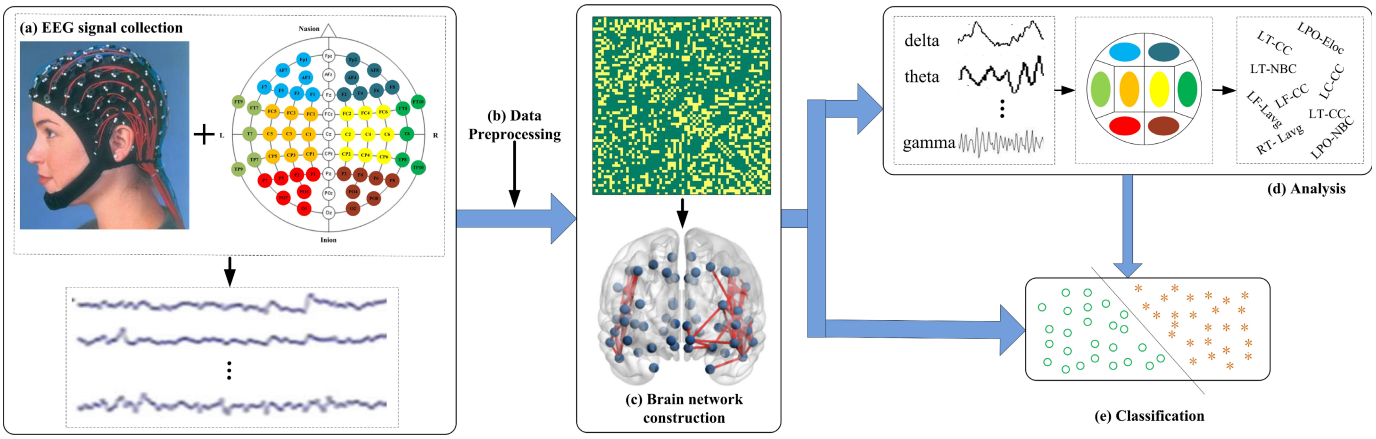

Fig. 1. Flowchart of the proposed method.

revealing the significance of inter-brain synchronization in group conflicts [33]. In aspect of classification is mainly based on modern machine learning techniques, the literatures [19] and [34] adopt various classification techniques to identify patients with mental illnesses, and compare the advantages and disadvantages of relevant classification technologies. The survey results clarify that patients with brain disease usually have abnormal in differences of EEG frequency bands, connection synchronization, differences of brain regions, etc. And the current representative classification methods are mostly based on modern machine learning technology. Based on this, we launched the subsequent analysis of the brain function network and classification of MDD patients.

Although some successes have been achieved for the analysis and classification of MDD, the existing research is far from up-to-date. In particular, the traditional EEG feature-level based MDD analysis and classification methods tend to pay more attention to the results of EEG feature selection and classification accuracy, while ignoring the correlation between EEG electrodes. To remedy these weaknesses of existing solutions, this article proposes a framework for MDD analysis and classification based on brain functional networks of resting-state EEG data. The contributions of this article are summarized as follows:

(1) This study found that the power spectrum of MDD patients significantly increases in theta and alpha2 bands, which supports the enhancement theory of negative brain activity in specific EEG bands of patients with MDD from the perspective of energy change.

(2) Synchronization analysis based on the PLI, this study found that the synchronization of MDD patients group had significantly higher compared to control group, especially in left frontal, left central, left temporal, left parietal-occipital, and right temporal in theta or alpha2 bands. This phenomenon may indicate that abnormal information processing in the brain of patients with MDD

(3) Analysis by relationship between network metrics with PHQ-9 scores, as well as area under receiver operating characteristic curve (AUC) of these metrics between MDD group and control group, and classification accuracy based on these metrics, we found that average shortest path length and clustering coefficient in left central region of theta band and node betweenness centrality in right parietal-occipital region may be served as potential biomarkers to effectively distinguish MDD from controls.

The remainder of this article is organized as follows. In Section II, we give the structure diagram of this study, introduces the experimental material, and a brain functional network framework is proposed for MDD of analysis and classification based on resting state EEG. In Section III, detailed statistics and analysis strategies, and classification algorithm used in this study are introduced. In Section IV, several experimental results are obtained. In Section V, relevant experimental results as well as advantages and disadvantages of our method are discussed. Finally, the limitations, disadvantage, and conclusion are presented in Sections VI and VII.

II. Materials and Methods

To clarify the idea of this article, Fig. 1 shows a flowchart of the proposed method. Its simplified process is as follows: (a) Resting state EEG signals were collected on 64 electrodes for about 5 minutes. (b) EEG data were preprocessed by eliminating EOG, filtering, and so on. (c) Brain function network was constructed based on PLI. (d) Design various methods to analyze the brain function network, and then obtain potential biomarkers that can effectively distinguish MDD from control group. (e) Classification of MDD and healthy controls..

A. Subjects

All subjects involved in the research were screened by screening tools, which were jointly developed by psychiatrists and researchers of "973 National Key Research and Development Program" according to international general scale. The international general scale includes: Patient Health Questionnaire 9-item (PHQ-9) [35], Generalized Anxiety Disorder 7-item (GAD-7) [36], Life Event Scale (LES) [37], Pittsburgh Sleep Quality Index (PSQI) [38]. Screening tools were used to investigate other physical and mental illnesses to ensure that the differences between the subjects were mainly caused by MDD. Finally, the experiment subjects were determined by psychiatrists based on screening tools and inclusion criteria. The inclusion criteria as follows:

MDD group: the psychiatrist's diagnosis was MDD and PHQ-9 score was greater than or equal to 5, and the subject did not take any psychotropic drugs within 2 weeks.

Control group: the psychiatrist's diagnosis was healthy, and all international general scales results were normal.

In addition, all subjects must also meet the following inclusion criteria: the ages of 18-55 years old, primary school education or above, normal intellectual activities, and no head injuries in the past. After meeting the inclusion criteria and signing informed consent by subjects or their family members, the subjects can participate in the experiment.

The initial experiment 24 subjects with MDD (male/female = 13:11, right-handed) were recruited from Lanzhou University Second Hospital, China, and 29 age-matched and education-matched healthy control were recruited (male/female = 20:9, right-handed) from the society [39]. To ensure gender-matched, this study only used data from 24 subjects with MDD (MDD group) and 24 health controls (Control group), and the sex ratio was 13:11. The mean and standard deviation of PHQ-9 score in MDD group was 18.33±3.50, and control group was 2.58±1.79 ($F = 10.162$, $p<0.001$), which indicate that the difference in research data was mainly due to MDD, rather than other factors.

B. Data and Preprocessing

All experimental data were recorded in a special room with quiet, no strong light, moderate temperature and humidity, good ventilation, and no electromagnetic interference. Subjects need to sit on a wooden chair in their own comfortable way and resting state. Simultaneously, In order to reduce the noise of electrooculography (EOG) and electromyography (EMG), subjects need to reduce or even avoid eye and body movements as much as possible. Then EEG signals were recorded for approximately five minutes by a 128-channel HydroCel Geodesic Sensor Net and Net Station software with Cz reference and 250 Hz sampling rates, which were positioned according to international standard 10-20 system. On the basis of ensuring the uniform distribution of electrodes and the effectiveness of the study, to control and reduce the amount of calculation, we only selected 64 electrodes of them and their reference electrode Cz. The selection and distribution of specific electrodes are shown in Fig. 1 below.

A lot of noise was inevitably being introduced in the process of EEG recording. To obtain relatively pure and more effective EEG data, it is necessary to preprocess the raw EEG signal. Usually depression-related EEG signals mainly exist in 0.5 Hz to 50 Hz [40]. So a band pass filter with a low cut-off frequency of 0.5 Hz and a high cut-off frequency of 50 Hz was adopted to eliminate low frequency drift and high-frequency noise. Electrooculography (EOG) was the most serious noise in EOG acquisition process [41]. Even if the subject in the resting state with eyes closed, the amplitude of EEG produced by blinking was more than ten times that of EEG. Therefore, this study uses a model based on adaptive noise cancellation and discrete wavelet transformation [42], [43] to remove EOG noise to obtain relatively pure EEG data.

C. Power Spectrum

The power spectrums of all EEG frequency bands were computed by Fast Fourier Transform (FFT) with a frequency resolution of 1/4 s = 0.25 Hz. Due to frequency resolution = fs/N and fs = 250Hz, that is, the number of sampling points is 1000. In this study, FFT is applied to explore alterations of power spectrum of MDD patients in different frequency bands. So as to find the abnormal of brain function connection. In order to obtain accurate experimental results, the absolute power values were computed in the following frequency bands: delta (0.5-4 Hz), theta (4-8 Hz), alpha1 (8-10Hz), alpha2 (10-13 Hz), beta1 (13-18 Hz), beta2 (18-21 Hz), beta3 (21-30 Hz) and gamma (30-48 Hz).

D. PLI and Construction of Brain Functional Matrices

The network consists of nodes and edges between nodes. In this study, each EEG electrode is defined as a node, and the connection strength between nodes is defined as edge. To avoid the volume conductor effect, PLI was used to calculate the connection strength between nodes. For any pair of EEG signals $x_j(t)$ and $x_k(t)$, the phase difference at time t can be expressed as:

$$|\Delta\varphi_{n,m}(t)| = |n\varphi_j(t) - m\varphi_k(t)| \tag{1}$$

where n and m are integers, generally the value of n and m are both 1 in neuroscience applications. $\varphi_j(t)$ and $\varphi_k(t)$ denotes the instantaneous phase of signals $x_j(t)$ and $x_k(t)$, which is calculated as follows:

$$\varphi_j(t) = \arctan\frac{\tilde{x}_j(t)}{x_j(t)} \tag{2}$$

$\tilde{x}_j(t)$ is the Hilbert transformation [44] of $x_j(t)$, defined as follows:

$$\tilde{x}_j(t) = \frac{1}{\pi}PV\int_{-\infty}^{\infty}\frac{x_j(\xi)}{t-\xi}d\xi \tag{3}$$

Here PV refers to cauchy principal value. Then the PLI value between the two signals $x_j(t)$ and$x_k(t)$ can be defined as:

$$PLI_{jk} = \left|\frac{1}{L}\sum_{l=0}^{L-1}\text{sign}(\Delta\varphi(t_l))\right|, \quad 0 \le PLI_{jk} \le 1 \tag{4}$$

L is the number of samples and sign is the signum function.

In this study, adjacency matrix was constructed by calculating PLI between EEG channels and then to draw the brain function network. All the functional connectivity matrices were calculated each 4 seconds with a 2 seconds overlapping window in different frequency band. Next, we average the functional connection matrix of MDD group and control group in each frequency band, and obtain two adjacency matrices C_{ij} of $64 * 64$.

$$C_{ij} = \begin{bmatrix} C_{11} & \cdots & C_{1n} \\ \vdots & \ddots & \vdots \\ C_{n1} & \cdots & C_{nn} \end{bmatrix}_{64*64} \tag{5}$$

E. Binarization of Brain Functional Network

Illustration of complex network theory based on graph theory that small world network can be characterized by smaller average shortest path length and higher clustering coefficient. So we calculated the following small world properties to realize binary brain network.

Average shortest path length: shortest path L_{ij} is the path with the least edges between any two nodes i and j. Edge length of weight network is defined as the reciprocal of the edge weight:

$$L_{ij} = \frac{1}{w_{ij}} \tag{6}$$

where w_{ij} is the connection weight between nodes i and j, that is, C_{ij} of the adjacency matrix. Average shortest path length of weight network (L_w) can be defined as:

$$L_w = \frac{1}{N(N-1)} \sum_{i=1,i\neq j}^{N} L_{ij} \tag{7}$$

N is the number of nodes in the weighted network.

Clustering coefficient: it is the probability that the neighbors of a node are neighbors of each other, which is an important parameter to measure the degree of network collectivization. Clustering coefficient of node i in weight network can be described as:

$$C_i = \frac{\sum_{j,k,j\neq k} w_{ij} w_{ik} w_{jk}}{\sum_{j,k,j\neq k} w_{ij} w_{ik}} \tag{8}$$

Here w_{ij}, w_{ik}, w_{jk} are also C_{ij}. Network clustering coefficient (C_w) is the average of C_i:

$$C_w = \frac{1}{N} \sum_{i=1}^{N} C_i \tag{9}$$

Small-world index: with random network act as the benchmark, discuss the small-world characteristics of the network and it can be defined as:

$$\sigma = \frac{C_w / C_{rand}}{L_w / L_{rand}} \tag{10}$$

In this study, C_{rand} and L_{rand} are the mean for average shortest path and clustering coefficient of 50 random networks with the same scale as the original network, respectively.

There are a large number of weak connections and pseudo connections in brain functional networks, and these links often blur the topology of core connections. So as to solve this problem binarization method based on threshold may be one of the best candidates to remove the weak connections. Considering there is currently no method for uniformly defining thresholds and starting from specific issue of this study, we have formulated a threshold binarization method based on $\sigma_{MDD}/\sigma_{control}$. This ratio was calculated between the MDD group and the control group among the 400 thresholds, where the threshold varies from 0.1 to 0.9 in steps of 0.002, and the threshold with the most significant difference of ratio acts as the binary threshold. Finally, it is found that threshold value is 0.26 (t-test, $p<0.001$) with the most significant difference between the two groups by statistics and analysis. Note that this binary method based on small world index ratio was supported and verified by previous studies on brain functional network [45].

III. Statistics And Analysis

A. Analysis of EEG Absolute Power in Different Frequency Bands

Many studies have shown that many mental disorders were closely related to low-frequency EEG signal [46]. To quickly find which frequency bands contain information significantly related to MDD, the absolute power averaged across all channels were calculated in each frequency within range of 0.5-48 Hz for two groups respectively.

B. Connection Synchronization Analysis Based on PLI

In order to explore which brain regions of MDD group have abnormal alterations of brain functional topological architecture compared with control group. We compare and analyze the differences of connection synchronization between two groups in binary brain network. When the threshold value was 0.26, the binary adjacency matrix of MDD group and control group was calculated based on PLI. Then a difference matrix was obtained by binary adjacency matrix of MDD group to subtract binary adjacency matrix of control group. The difference matrix was used to construct brain functional network, and then analyze the connection synchronization difference between different brain regions.

C. Analysis of Brain Functional Network Metrics in Different Brain Regions

Small world network has relatively high local efficiency and global efficiency in the process of information transmission and processing [47].This discovery triggered another study upsurge of brain network. Many studies have clarified from an anatomical perspective that brain connectivity is considered to simultaneously coordinate the opposing requirements of functional integration and segregation. It is generally believed that such a brain tissue reflects the optimal balance of functional integration and segregation. Furthermore, brain functional network can be characterized by different metrics. Based on this consideration, the integration and segregation metrics of brain function network were calculated and used to analyze the difference between MDD group and control group for binary network. A list of these small world based network metrics is shown in Table I.

Exploring region where brain function topological architecture has alteration, we analyzed the differences between MDD group and the control group in the above network metric. Analysis of variance (ANOVA) was used to complete this task. EEG analysis based on brain region originated from the research of brain function changes during adolescence [48]. In this study, we averaged the network metrics of each subject in eight non-overlapping brain regions. Fig. 2 lists the segmentation of these brain regions.

D. Discrimination Ability of Network Metrics and Potential Biomarker

To determine whether the network metrics have the ability to distinguish MDD from controls, and whether they can be potential biomarkers to identify MDD, the correlation between

TABLE I
LIST OF NETWORK METRICS BASED ON SMALL WORLD.

Abbreviation	Formula	Description
L_{avg}	$L_{avg} = \frac{1}{N(N-1)}\sum_{i=1,i\neq j}^{N} L_{ij}$	L_{ij} is the shortest path between nodes i and j. N is the number of node in the network.
NBC	$NBC_i = \frac{1}{(N-1)(N-2)}\sum_{i\neq j,i\neq h,j\neq h}\frac{\rho_{jh}(i)}{\rho_{jh}}$	ρ_{jh} is the number of shortest path between nodes j and h, and $\rho_{jh}(i)$ is the number of shortest path between nodes j and h that pass through i.
E_{glo}	$E_{glo} = \frac{1}{N(N-1)}\sum_{i,j\in V,i\neq j} L_{ij}$	V is the node set of the network, N is the number of node in the network.
CC	$CC = \frac{1}{N}\sum_{i=1}^{N} C_i = \frac{1}{N}\sum_{i=1}^{N}\frac{2e_i}{k_i(k_i-1)}$	C_i is the clustering coefficient of node i, k_i is the degree of node i, and e_i is the number of triangles formed by the adjacent nodes of node i.
E_{loc}	$E_{loc} = \frac{1}{N}\sum_{i\in V} E(i) = \frac{1}{N}\sum_{i\in V}\frac{\sum_{j\neq h\in V_i}[L_{jh}(i)]^{-1}}{e_i(e_i-1)}$	E(i) is the local efficiency of node i, and $L_{jh}(i)$ is the length of the shortest path between node j and h, that contains only neighbors of node i.

NOTE: (1) L_{avg}: average shortest path length, NBC: node betweenness centrality, E_{glo}: glocal efficiency, CC: clustering coefficient, E_{loc}: Local efficiency. (2) Integration metric include: L_{avg}, NBC, and E_{glo}. Segregation metric include: CC and E_{loc}.

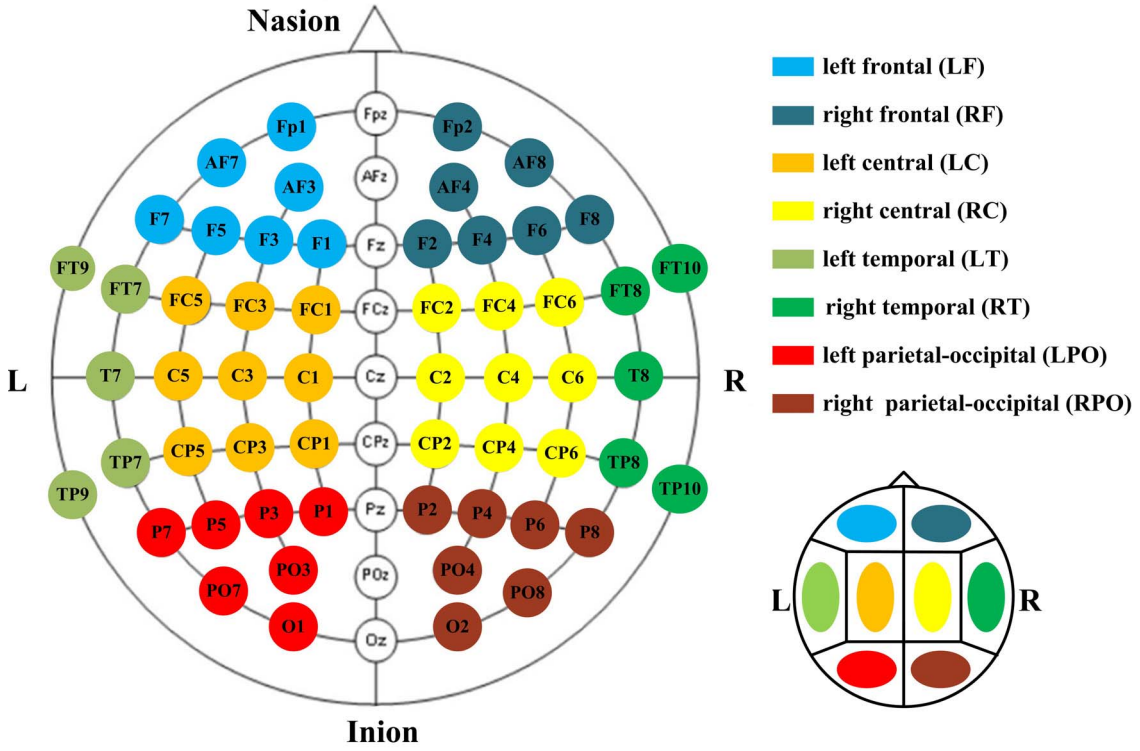

Fig. 2. Segmentation of eight non-overlapping brain regions.

the significantly network metrics in significantly different regions and PHQ-9 scores were analyzed within MDD and controls. Pearson correlation coefficient was employed in this analysis.

E. Evaluation and Classification

To further evaluate whether network metrics having significant correlation with PHQ-9 scores served as potential biomarker can effectively classify MDD from controls, we adopt the following four representative algorithms as classification tools to verify [49]: random forest (RF, numTrees=20) based on ensemble learning, support vector machine (SVM, Linear Kernel) based on statistical learning, K-nearest neighbor (KNN, K=3) based on distance, artificial neural network (ANN, activation function is Sigmoid) based on mathematical model to simulate neurons. That is, these potential biomarkers serve as inputs to the four classifiers. To obtain an unbiased and statistically significant result, the classifier was executed with 10-fold cross validation. The classification performance was quantified and evaluated using accuracy, sensitivity (recall), specificity, precision, F1-score, False alarm rate and Cohen's Kappa.

$$\text{Accuracy} = \frac{TP + TN}{TP + TN + FP + FN} \tag{11}$$

$$\text{Sensitivity} = \frac{TP}{TP + FN} \tag{12}$$

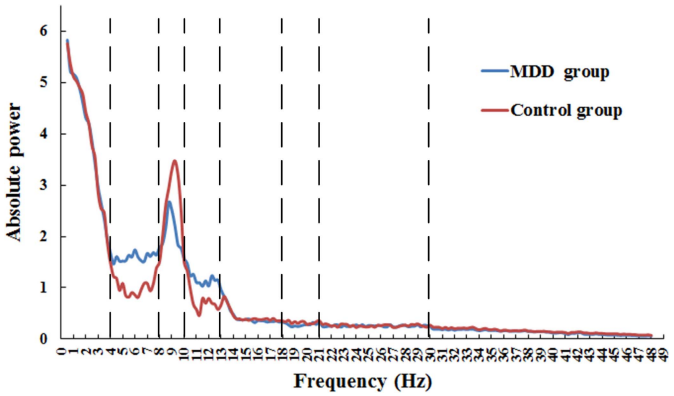

Fig. 3. Average of absolute power between MDD group and control group.

$$\text{Specificity} = \frac{\text{TN}}{\text{TN}+\text{FP}} \tag{13}$$

$$\text{Precision} = \frac{\text{TP}}{\text{TP}+\text{FP}} \tag{14}$$

$$\text{F1\_score} = 2 * \frac{\text{precision} * \text{recall}}{\text{precision} + \text{recall}} \tag{15}$$

$$\text{False\_alarm\_rate} = \frac{\text{FP}}{\text{FP}+\text{TN}} \tag{16}$$

$$\text{Cohen's\_kappa} = 2 * \frac{\text{TN} * \text{TP} - \text{FP} * \text{FN}}{(\text{TN}+\text{FN}) * (\text{FN}+\text{TP}) + (\text{FP}+\text{TP}) * (TN+FP)} \tag{17}$$

where

True Positive (TP): number of MDD classified correctly by the proposed method as MDD.

False Positive (FP): number of healthy control classified incorrectly by the proposed method as MDD.

True Negative (TN): number of healthy control classified correctly by the proposed method as healthy control.

False Negative (FN): number of MDD classified incorrectly by the proposed method as healthy control.

IV. Results

A. MDD-Related Frequency Band

A line diagram of frequency-power relationship is shown in Fig. 3. Both MDD group and control group exhibited higher absolute power in the alpha1 frequency band (8-10 Hz), but there is no significant difference in the change regularity between two groups. In the six frequency bands such as delta, alpha1, beta1, beta2, beta3, gamma frequency bands, the absolute power change regularity between two groups was almost the same. However, absolute power of MDD group is significantly higher than control group in theta frequency band (4-8 Hz) and alpha2 frequency band (10-13 Hz), and the change regularity was obviously inconsistent.

B. MDD-Related Brain Regions

Due to the difference yielded from absolute power analysis was not obvious in delta, alpha1, beta1, beta2, beta3, gamma bands, our further research focuses paid more on theta and alpha2 bands. PLI were calculated for each pair of channels on the scalp, and the corresponding binary adjacency matrices were generated with 0.26 as the threshold, as shown in Fig. 4. The adjacency matrices of both groups in theta and alpha2 bands showed complex but rather simple connection patters, with various channel regions have different synchronization levels, such as yellow indicates high synchronization and green indicates low synchronization. Compared with the control group, MDD patients had more enhanced synchronization between the EEG channels. However, it is not easy to quickly and clearly find the synchronization difference between groups from Fig. 4.

To this end, we calculated the difference matrix between the groups, and plotted a 3D graph of the difference matrix based on the position of the corresponding electrode in the scalp, as shown in Fig. 5. The 3D graph of brain function connection clearly shows the difference between the two groups in theta and alpha2 bands. In the theta frequency band, except for a few links in LT and RT regions, most of the links were distributed in the rest regions of the left hemisphere. In the alpha2 frequency band, except for a few links in LF and LPO regions, most of the links were distributed in two temporal regions. The results of the PLI-based synchronization analysis and distribution of brain function connection showed that the MDD group had significantly higher synchronization in the left hemisphere of the brain, especially in LF, LT, and LPO regions, and slightly higher in the right hemisphere of the brain such as RT region, compared with control group in the theta or alpha2 bands.

C. MDD-Related Binary Network Metrics

Based on the results of the previous subsection, we further analyzed the differences of network metrics of LF, LC, LT, LPO, and RT in the theta band, and LF, LT, LPO, and RT in the alpha2 band. The analysis results were shown in Figs. 6 and 7. For the theta band (see Fig. 6), we can observe the following differences, which are: NBC in LT region, CC in LF and LC regions, and E_{loc} in LPO region decreased significantly in MDD group, compared with control group. But MDD group showed significant increase in L_{avg} when LC region. For the alpha2 band (see Fig. 7), compared with control group, L_{avg} in LF and RT regions increased significantly in MDD group. Otherwise MDD group showed significant decrease in NBC and CC when LPO and LT, respectively. However, there was no significant difference between two groups in the network metrics of other brain regions in the theta and alpha2 bands.

D. MDD-Related Potential Biomarker and Effectiveness

According to Figs. 6 and 7, we can conclude that LC-Lavg, LT-NBC, LF-CC, LC-CC and LPO-Eloc in theta band and LF-Lavg, LPO-NBC, LT-CC and RT- Lavg in alpha2 band had significant differences between MDD group and control group.

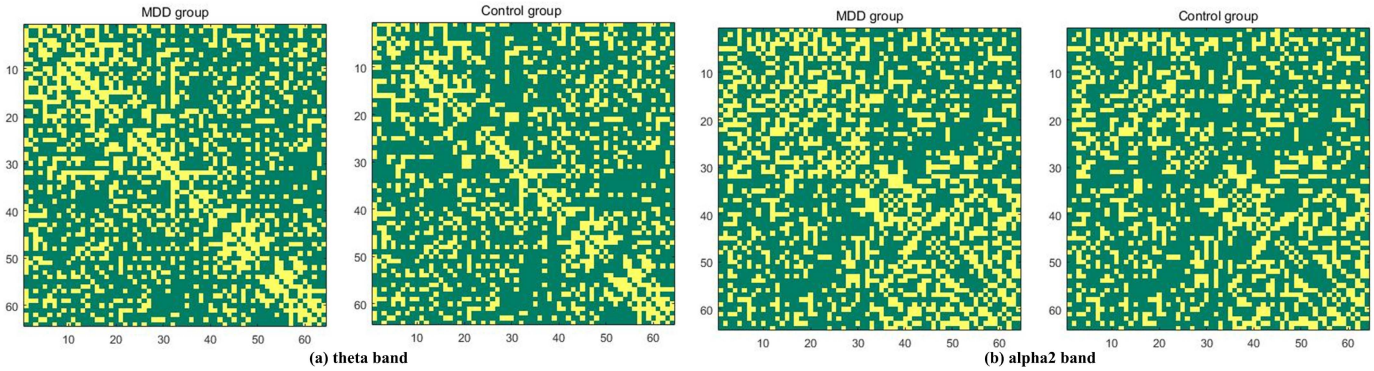

Fig. 4. PLI-based binary adjacency matrices with 0.26 as the threshold, in these 64∗64 matrix graph, the cross color points at each horizontal and vertical axis represent the PLI of two corresponding channels. (a) Binary adjacency matrix of theta band. (b) Binary adjacency matrix of alpha2 band.

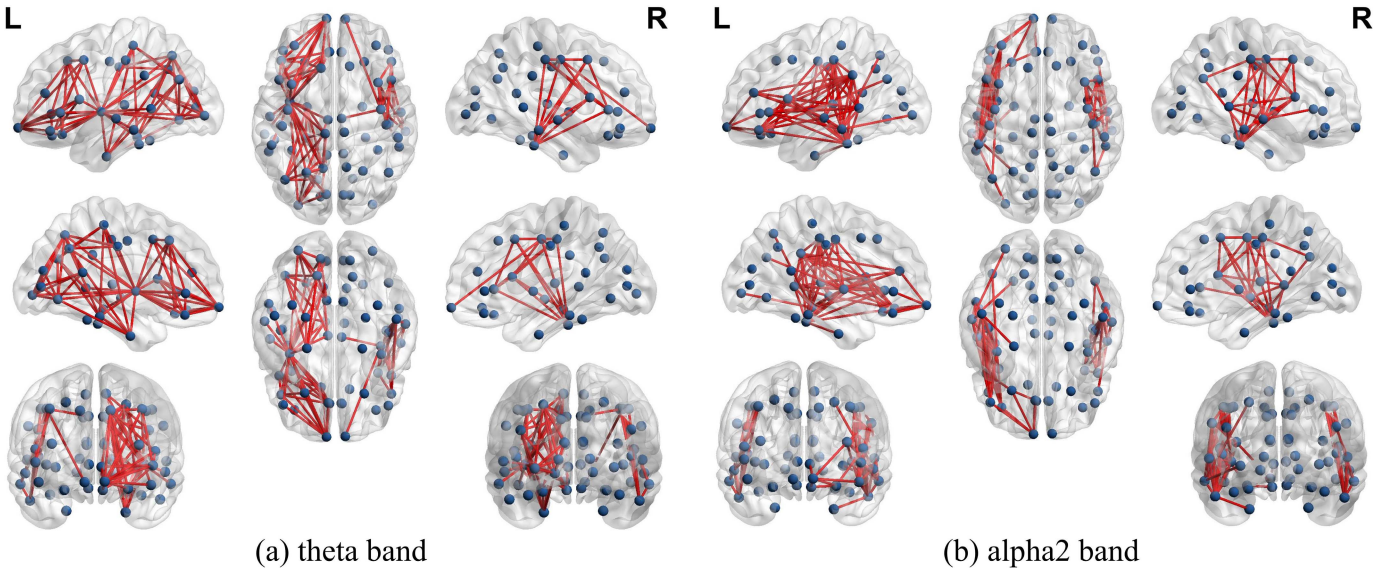

Fig. 5. The scalp position distribution of the difference matrix in (a) theta and (b) alpha2 bands. The dark blue nodes represent 64 electrodes, and the red lines represent the binarization results between the nodes.

On this basis, to achieve the purpose of exploring the potential biomarkers that can effectively detect MDD. We further evaluated the relationship these network metrics and PHQ-9 scores, using Pearson correlation analysis. Moreover, we also assessed the ability of these metrics to distinguish MDD patients from control group using AUC.

Results are in Figs. 8 and 9. For theta band, L_{avg} and CC in the LC region were negatively correlated with the scores of PHQ-9 ($p<0.05$), AUC value were 0.839 and 0.788 respectively (see Figs. 8(a) and 8(d)). Besides, other significant network metrics in theta band were either marginally correlation or no correlation with PHQ-9, or AUC value is less than 0.70, which as shown in Figs. 8(b) and 8(c), NBC in the LT region and CC in the LF region showed marginally correlation with PHQ-9 scores ($0.05<p<0.1$). Nevertheless, E_{loc} in the LPO region showed no correlation with PHQ-9 scores ($p > 0.1$), and AUC value was less than 0.70 (AUC = 0.561) as shown in Fig. 8(f).

For alpha2 band, Figs. 9(b) and 9(c) showed that L_{avg} and NBC were correlated to the scores of PHQ-9 ($p<0.05$) in the RT and LPO regions respectively, as well as AUC values were 0.864 and 0.815. Although L_{avg} in the LF region were correlated with PHQ-9 scores, AUC value was less than 0.70 (see Fig. 9(a)). There were marginally significant correlations between CC in the LT region and PHQ-9 scores ($p = 0.067$, $0.05<p<0.1$) as shown in Fig. 9(d).

In order to verify whether these network metrics (LC-L_{avg} and LC-CC in theta band, and RT-L_{avg} and LPO-NBC in the alpha2 band) that were significantly correlation with PHQ-9 score and have a high AUC value were effectives as MDD-related potential biomarker, and can be able to detected MDD from control group. MDD-related potential biomarkers from inter-subject data were performed 10-fold cross validation based on RF, SVM, KNN and ANN, that is, MDD-related potential biomarkers as mixing feature for the input of above four classifiers. The results of classification accuracy were shown in Table II, and the highest classification accuracy is 89.25% of RF. Meanwhile, Fig. 10 lists the synthesis of RF seven indexes such as accuracy, sensitivity (recall), specificity, precision, F1-score, False alarm rate and Cohen's Kappa. LC-L_{avg} and LC-CC in theta band, and RT-L_{avg} and LPO-NBC in the alpha2 band were together

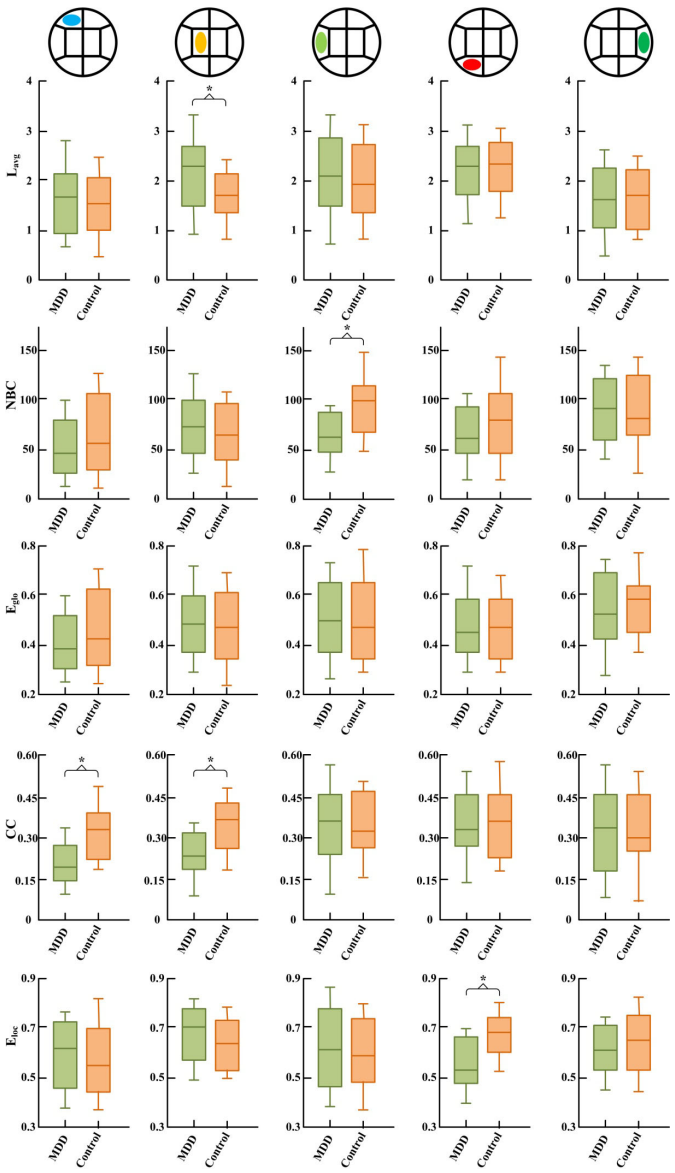

Fig. 6. Statistical analysis result of five network metrics in different brain regions of theta band. The center line of the box plot represents the median value, and the asterisk (∗) represents a significant difference ($p<0.05$, one-way ANOVA). Each row represents the difference analysis result of one metric in five brain regions.

TABLE II
RESULTS OF CLASSIFICATION ACCURACY BASED ON FOUR CLASSIFIERS.

	RF	SVM	KNN	ANN
Accuracy	89.25%	74.98%	84.53%	85.14%

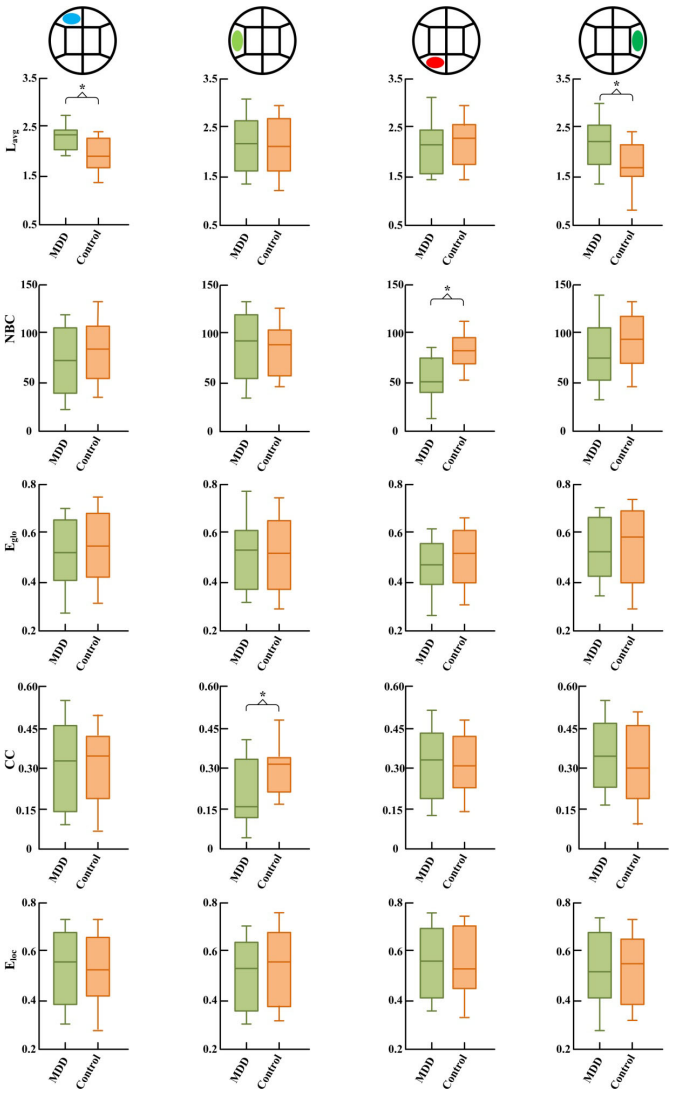

Fig. 7. Statistical analysis result of five network metrics in different brain regions of alpha2 band. Each row represents the difference analysis result of one metric in four brain regions.

TABLE III
AVERAGE PERFORMANCE OF EACH NETWORK METRIC AS POTENTIAL BIOMARKER.

	theta		alpha2	
	LC-L_{avg}	LC-CC *	RT-L_{avg}	LPO-NBC
Accuracy	87.96%	93.31%	83.73%	90.77%
Sensitivity	94.59%	95.76%	87.91%	93.65%
Specificity	81.33%	90.85%	79.54%	87.89%

Asterisk (*) result is best result.

used as input, the lowest classification accuracy obtained by 10-time cross validation was 85.62%, its sensitivity, specificity, precision, F1-score, False alarm rate and Cohen's kappa were 88.91%, 82.35%, 89.02%, 88.96%, 0.31% and 0.76, respectively (see Fig. 10: Fold-1), the highest classification accuracy obtained by 10-time cross validation was 93.16%, its sensitivity, specificity, precision, F1-score, False alarm rate and Cohen's kappa were 95.69%, 90.62%, 95.13%, 95.41%, 0.81% and 0.90, respectively (see Fig. 10: Flod-4), the average classification accuracy of 10-time cross validation was 89.25%. So these four network metrics together as potential biomarkers can effectively distinguish MDD from controls. In addition, we also analyzed the effectiveness of each network metric as potential biomarker and the experimental results were presented in Table III, which provided the average performance of different network metrics for detecting MDD. As can be seen

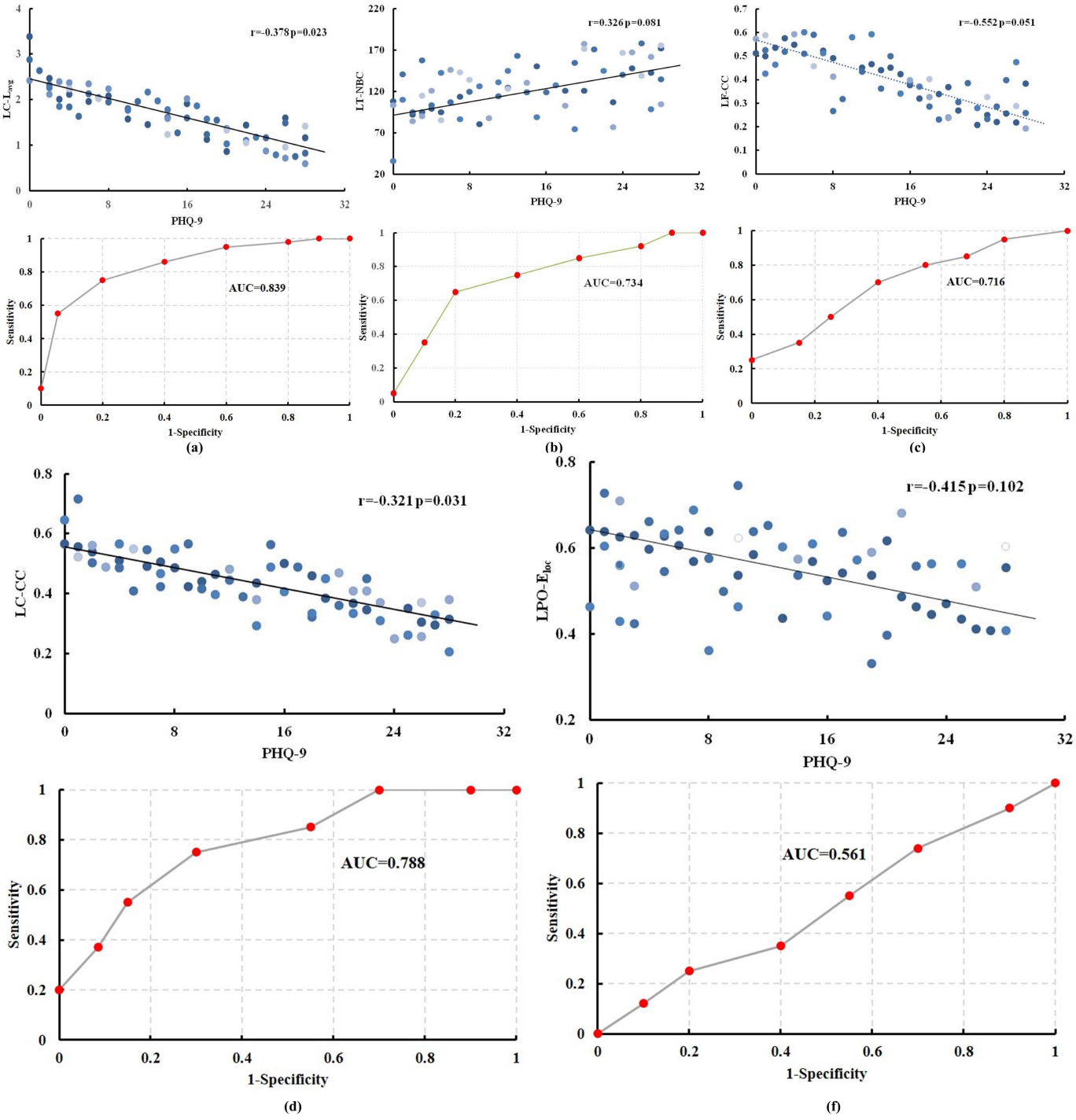

Fig. 8. The relationship between significant network metrics with PHQ-9 scores, as well as AUC of these metrics between MDD group and control group in theta frequency band. (a) LC-L_{avg}, (b) LT-NBC, (c) LF-CC, (d) LC-CC, (f) LPO-E_{loc}. Note: AUC$<$0.70 means that poor performance of diagnostic test.

from the Table III, the ability of the four network metrics as potential biomarkers to distinguish MDD from control group was in the order of strong to weak: LC-CC (theta), LC-L_{avg} (theta), LPO-NBC (alpha2), RT-L_{avg} (alpha2).

V. Discussion

This study used power spectrum analysis found that the absolute power of MDD group was significantly higher than control group in theta and alpha2 bands, and the change regularity was inconsistent. The result reveals that the brain function structure of MDD patients has altered in these two bands. Several previous studies have reported the same or similar conclusions: abnormal brain function occurs in some specific frequency bands of MDD patients. From the perspective of structural synchrony index, Andrew *et al.* [50] clarified that impaired functional connectivity at EEG alpha and theta

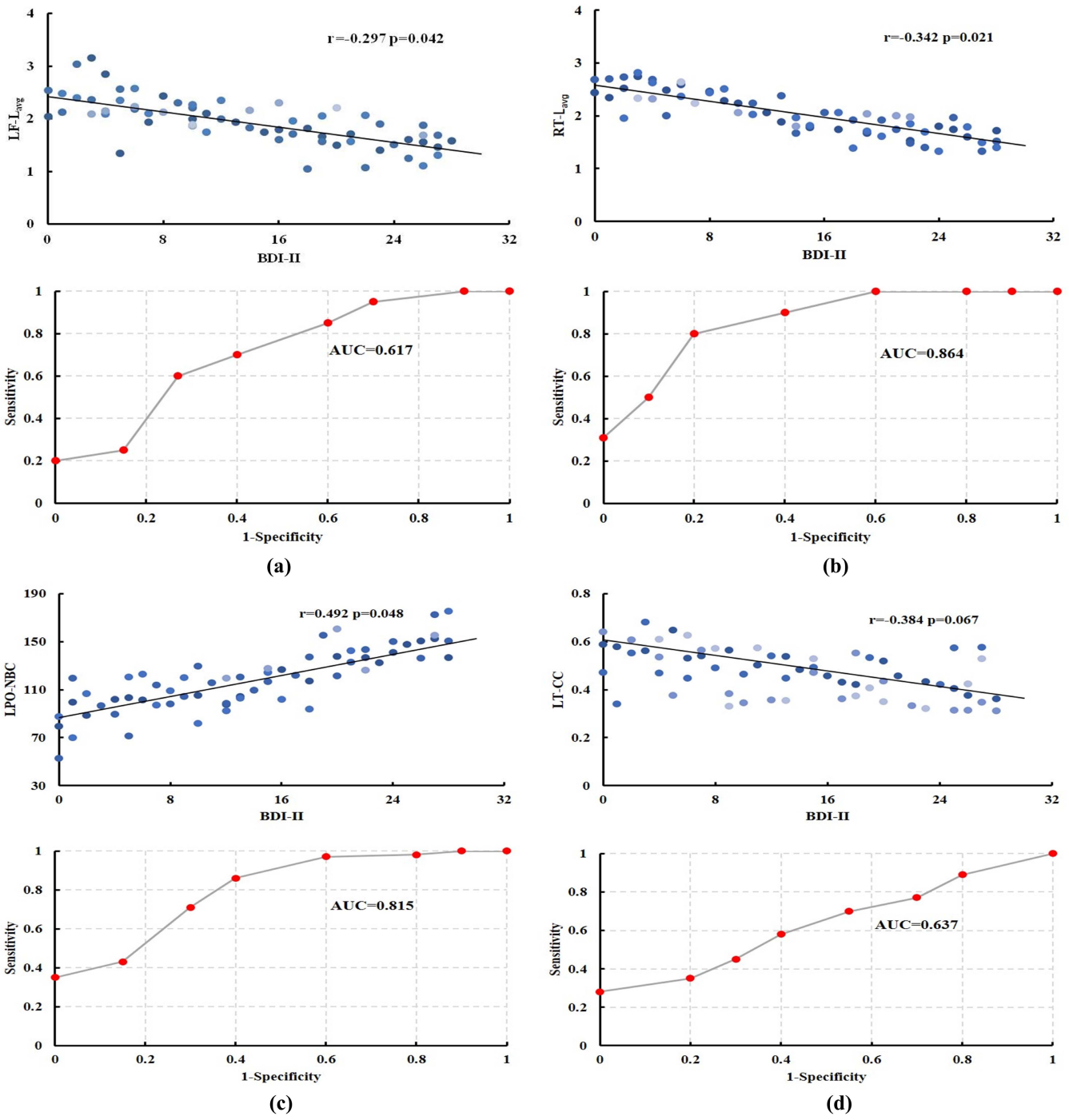

Fig. 9. The relationship between significant network metrics with PHQ-9 scores, as well as AUC of these metrics between MDD group and control group in alpha2 frequency band. (a) LF-Lavg, (b) RT-Lavg, (c) LPO -NBC, (d) LT-CC.

bands in MDD. The study of [51] explored resting state EEG in different frequency bands and found that MDD group had significantly higher coherence as compared to control group in the theta, alpha and beta bands. Similarly, the study of EEG by [52] also found that there was an abnormal power spectrum in theta and alpha bands, and study in [53] pointed to theta band asymmetry of EEG can be used as a potential biomarker to identify depression. However, there are overlaps and slight differences in alpha band between the results of this study and previous studies, which may be caused by the number of electrodes and subdivision of band. In addition, why are the specific EEG bands abnormal in patients with MDD? Some researchers interpret this phenomenon as strengthen of negative brain activity in specific EEG bands [54]. Our findings support this theory of increased brain activity from the perspective of energy change. Meanwhile, it also further confirms the vital role of theta and alpha2 bands in the study of MDD.

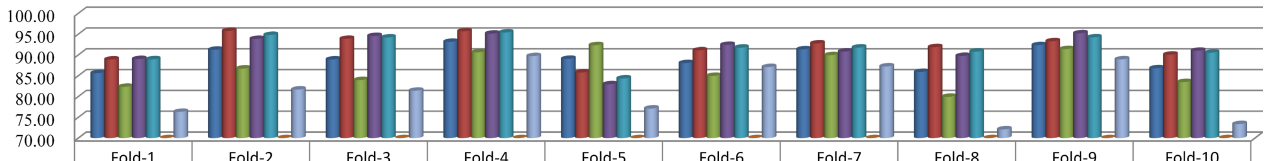

	Fold-1	Fold-2	Fold-3	Fold-4	Fold-5	Fold-6	Fold-7	Fold-8	Fold-9	Fold-10
Accuracy (%)	85.62	91.26	88.92	93.16	89.06	88.04	91.35	85.91	92.35	86.79
Sensitivity (%)	88.91	95.78	93.87	95.69	85.79	91.10	92.77	91.88	93.29	90.08
Specificity (%)	82.35	86.73	83.96	90.62	92.34	84.97	89.94	79.95	91.41	83.48
Precision (%)	89.02	93.86	94.56	95.13	82.95	92.42	90.81	89.76	95.21	91.01
F1-score (%)	88.96	94.81	94.21	95.41	84.35	91.76	91.78	90.81	94.24	90.54
False alarm rate (%)	17.65	13.27	16.04	9.38	7.66	15.03	10.06	20.05	8.59	16.52
Cohen's Kappa（%）	76.32	81.69	81.41	89.72	77.12	87.09	87.24	72.11	88.95	73.39

Fig. 10. Performance evaluation of MDD-related potential biomarkers (LC-L_{avg} and LC-CC in theta band, and RT-L_{avg} and LPO-NBC in the alpha2 band) based on RF classifier using 10-fold cross validation. Note: Fold-2 means that the second time cross validation, the remaining Fold-1 and Fold-3 to Fold-10 have the same meaning.

The research on the brain functional network of MDD patients has been extensively explored, and new research achievements continue to emerge. However, due to the differences on experimental methods and data analysis strategies, different or even opposite conclusions are obtained in MDD research based on brain function networks. For example, studies in [55], [56] found that increased brain functional connectivity in MDD patients, while decreased brain functional connection was reported in the study of [57]. In this article, we also studied the alteration of brain function connections of MDD based on PLI and difference matrix, and results showed that the synchronization of MDD patients group had significantly higher compared to control group, especially in the left hemisphere, such as LF, LC, LT, and LPO in theta and alpha2 bands. Aiming at the phenomenon of increased synchronization of MDD, we speculate that the brain information processing was abnormal in MDD patients. This conclusion was basically consistent with the research of Joormann's team [58] and Leistedt's team [59]. The ability of emotion regulation was obviously absent in MDD patients pointed out by Joormann's team, and the information processing problems of brain functional networks may underlie acutely depressive disease was reported by Leistedt's team. The higher synchronicity was found in the left hemisphere, we believe was attributed to the hemispheric asymmetry of information processing in MDD patients. Previous study [60] has confirmed that left hemisphere lateralization was a characteristic of dysfunction in MDD. Although synchronicity has a great contribution to revealing the inherent characteristics of MDD, it is necessary to further study the information processing mechanism of MDD to obtain more accurate conclusions.

Small-world network represents the best organizational structure in terms of cabling costs, local independence, global integration, reliability and so on [59]. Research on modeling and simulation shows that small-world network configuration facilitates synchronization between brain neurons and efficient information processing [61]. Contemporary scientific studies reveals that the brain structure network constructed using the structure and diffusion magnetic resonance imaging data and the brain functional network constructed using EEG or MEG data of healthy population have stable small-world characteristics, while the brain network constructed by data of people with mental illnesses usually exhibits the loss of small-world characteristics as "a randomization process". For example, in sleep brain functional networks, Leistedt *et al.* [59] pointed to functional reorganization of patients with depression lost small-world characteristics. Cammoun *et al.* [62] constructed the brain structure network of patients with schizophrenia and found that their small-world characteristics showed abnormal randomization of connection pattern. A shift toward randomization of brain networks in MDD group compared with controls group by reported by [63]. It is worth noting that this study also reached similar conclusions with the above-mentioned studies. In network metric with significant difference between MDD group and control group, our research results explain that MDD exhibited increased LC-L_{avg} in theta band and LF-L_{avg} and RT-L_{avg} in alpha2 band, as well as MDD exhibited decreased LF-CC and LC-CC in theta band and LT-CC in alpha2 band, which means that small-world characteristics of brain function network in MDD patients was weakened and tends to be randomized.

In addition, we found L_{avg} and CC of LC in theta band, and RT-L_{avg} and LPO-NBC in alpha2 band were significantly related to the PHQ-9 scores. Similar conclusions have been found in previous studies. The CC of the left amygdala was related to the scores of PHQ-9 in the study of [64]. Zhang *et al.* [65] suggested that NBC in the left hippocampus and caudate nucleus were significantly related to the severity of MDD. More importantly, the four network metrics (LC-L_{avg} and LC-CC in theta band, and RT-L_{avg} and LPO-NBC in the alpha2 band) were used individually or jointly as potential biomarkers to detect MDD from control group, the lowest and the highest, and the average accuracy was 83.73%, 93.31% and 89.25%, respectively. This result further confirmed the effectiveness of these potential biomarkers for the discrimination MDD patients from controls.

Due to the different in methods, datasets, and data usage strategies, it is difficult to fully reflect the advantages and disadvantages of various methods only based on classification accuracy. However, the advantages and disadvantages of various methods can be partially or indirectly reflected by comparing accuracy and other indicators. Based on this

TABLE IV
COMPREHENSIVE COMPARISON OF EXISTING STATE-OF-THE-ART METHODS WITH THE PROPOSED METHOD.

Studies	Subject	Channel	Method	Potential biomarker or feature	Accuracy
Cai et al. [2]	86 MDD and 92 NC	EEG (3 channels)	Feature-level fusion	60 linear EEG features and 36 nonlinear EEG features	86.98%
Peng et al. [3]	27 MDD and 28 NC	EEG (128 channels)	Multivariate pattern analysis	249 EEG features	92.73%
Zhang et al. [4]	81 MDD and 89 NC	EEG (3 channels) and voice (1 channel)	Multimodal fusion	6 EEG features and 15 voice features	86.64%
Cai et al. [15]	86 MDD and 92 NC	EEG (3 channels)	Case-Based Reasoning Model	113 EEG features	91.25%
Liu et al. [29]	20 MDD and 19 NC	EEG (64 channels)	SVM	3 potential biomarker	89.7%,
Cai et al. [37]	92 MDD and 121 NC	EEG (3 channels)	KNN	270 EEG features	79.27%
Zhang et al. [64]	13 MDD and 13 NC	EEG (64 channels)	Independent component analysis	-	-
Our work	24 MDD and 24 NC	EEG (64 channels)	Brain Functional Networks	LC-CC in theta band	93.31%

NC: normal controls, -: no such content.

consideration, Table IV lists a comprehensive comparison for existing state-of-the-art methods and our proposed method, including the number of subject, type and number of channel, research method, the number of potential biomarker or feature, and classification accuracy. So that readers can have a deeper understanding of the current status of related research fields.

VI. LIMITATION AND DISADVANTAGE

There are some limitations and disadvantages of the proposed method that need to be addressed in the future. First of all, the limited data contained in the dataset used in this study may be a shortcoming of this article. Although some conclusions obtained from this data were consistent with the previous relevant research, the information provided by the topological brain network is very limited due to the limited data. Therefore, it is necessary to continuously expand in future research the dataset to obtain more sufficient information about the changes of the brain function network topology in patients with MDD. Secondly, the conformation of biomarkers is a rigorous and complex process. However, to impress readers and make it easier to express in the article, this study found that LC-L_{avg} and LC-CC in theta band, RT-L_{avg} in alpha2 can effectively distinguish MDD from controls, so we call these three network metrics "potential biomarkers". In order to avoid misunderstanding, it is explained here. Besides, although EEG has high temporal resolution, its low spatial resolution makes the network topographical structure of these findings difficult to evaluate different cortical regions of patient with MDD.

VII. CONCLUSION

This study aims to explore the brain abnormal changes of MDD patients, a series of analysis were performed on brain function network based on resting state EEG data. It was found that the power spectrum of the MDD group significantly increased in the theta and alpha2 bands. On this basis, we investigated the alterations of brain structure of MDD patients based on PLI and difference matrix, and we found that brain synchronization was significantly increased of MDD group compared with the control group, especially in the left hemisphere, such as LF, LC, LT, and LPO. This finding suggests that the brain information processing of MDD patients was abnormal. We also found that MDD increased LC-L_{avg} in theta band and LF-L_{avg} and RT-L_{avg} in alpha2 band, as well as MDD decreased LF-CC and LC-CC in theta band and LT-CC in alpha2 band. The change trend of these network metrics often indicates that the brain functional network of MDD patients tend to randomize. In addition, the four network metrics of LC-L_{avg} and LC-CC in theta band, and RT-L_{avg} and LPO-NBC in the alpha2 band were significantly correlated with MDD levels, which show that these network metrics can be used as effective potential biomarkers to distinguish MDD from controls, and the highest accuracy can reach 93.31%.

REFERENCES

[1] J. Sayers, "The world health report 2001-Mental health: New understanding, new hope," *Bull. World Health Org.*, vol. 79, no. 11, p. 1085, Nov. 2001.
[2] H. Cai, Z. Qu, Z. Li, Y. Zhang, X. Hu, and B. Hu, "Feature-level fusion approaches based on multimodal EEG data for depression recognition," *Inf. Fusion*, vol. 59, pp. 127–138, Jul. 2020.
[3] H. Peng *et al.*, "Multivariate pattern analysis of EEG-based functional connectivity: A study on the identification of depression," *IEEE Access*, vol. 7, pp. 92630–92641, Jul. 2019.
[4] X. Zhang, J. Shen, Z. U. Din, J. Liu, G. Wang, and B. Hu, "Multimodal depression detection: Fusion of electroencephalography and paralinguistic behaviors using a novel strategy for classifier ensemble," *IEEE J. Biomed. Health Informat.*, vol. 23, no. 6, pp. 2265–2275, Nov. 2019.
[5] B. Zhang *et al.*, "Ubiquitous depression detection of sleep physiological data by using combination learning and functional networks," *IEEE Access*, vol. 8, pp. 94220–94235, 2020.
[6] Z. Yao *et al.*, "Morphological changes in subregions of hippocampus and amygdala in major depressive disorder patients," *Brain Imag. Behav.*, vol. 14, no. 3, pp. 653–667, Dec. 2018.
[7] M. A. M. Hernández, A. F. Lucas, R. Hornero, and P. Zuluaga, "P01-70-Complexity analysis of brain's activity in major depression using magnetoencephalography (MEG)," *Eur. Psychiatry*, vol. 25, pp. 291–300, Jul. 2010.
[8] X.-J. Li and G.-H. Yang, "Graph theory-based pinning synchronization of stochastic complex dynamical networks," *IEEE Trans. Neural Netw. Learn. Syst.*, vol. 28, no. 2, pp. 427–437, Feb. 2017.
[9] Y. He and A. Evans, "Graph theoretical modeling of brain connectivity," *Current Opinion Neurol.*, vol. 23, no. 4, pp. 341–350, 2010.
[10] Z. Sha, T. D. Wager, A. Mechelli, and Y. He, "Common dysfunction of large-scale neurocognitive networks across psychiatric disorders," *Biol. Psychiatry*, vol. 85, no. 5, pp. 379–388, Mar. 2019.

[11] H. Yu, X. Lei, Z. Song, C. Liu, and J. Wang, "Supervised network-based fuzzy learning of EEG signals for Alzheimer's disease identification," *IEEE Trans. Fuzzy Syst.*, vol. 28, no. 1, pp. 60–71, Jan. 2020.

[12] A. Babajani and H. Soltanian-Zadeh, "Integrated MEG/EEG and fMRI model based on neural masses," *IEEE Trans. Biomed. Eng.*, vol. 53, no. 9, pp. 1794–1801, Sep. 2006.

[13] A. A. Fingelkurts, A. A. Fingelkurts, and S. Kahkonen, "Functional connectivity in the brain—Is it an elusive concept?" *Neurosci. Biobehav. Rev.*, vol. 28, no. 8, pp. 827–836, Jan. 2005.

[14] S. Siuly, Y. Li, and Y. C. Zhang, "Electroencephalogram (EEG) and Its Background," in *EEG Signal Analysis and Classification: Techniques and Applications* (Health Information Science). Cham, Switzerland: Springer Nature, 2016, pp. 3–14.

[15] H. Cai, X. Zhang, Y. Zhang, Z. Wang, and B. Hu, "A case-based reasoning model for depression based on three-electrode EEG data," *IEEE Trans. Affect. Comput.*, vol. 11, no. 3, pp. 383–392, Jul. 2020.

[16] G. Fraga González *et al.*, "Graph analysis of EEG resting state functional networks in dyslexic readers," *Clin. Neurophysiol.*, vol. 127, no. 9, pp. 3165–3175, Sep. 2016.

[17] M. Rubinov *et al.*, "Small-world properties of nonlinear brain activity in schizophrenia," *Hum. Brain Mapping*, vol. 30, no. 2, pp. 403–416, Feb. 2009.

[18] H. Yu, X. Li, X. Lei, and J. Wang, "Modulation effect of acupuncture on functional brain networks and classification of its manipulation with EEG signals," *IEEE Trans. Neural Syst. Rehabil. Eng.*, vol. 27, no. 10, pp. 1973–1984, Oct. 2019.

[19] S. Siuly *et al.*, "A new framework for automatic detection of patients with mild cognitive impairment using resting-state EEG signals," *IEEE Trans. Neural Syst. Rehabil. Eng.*, vol. 28, no. 9, pp. 1966–1976, Sep. 2020.

[20] A. F. Leuchter, I. A. Cook, A. M. Hunter, C. Cai, and S. Horvath, "Resting-state quantitative electroencephalography reveals increased neurophysiologic connectivity in depression," *PLoS ONE*, vol. 7, no. 2, Feb. 2012, Art. no. e32508.

[21] C. J. Stam, G. Nolte, and A. Daffertshofer, "Phase lag index: Assessment of functional connectivity from multi-channel EEG and MEG with diminished bias from common sources," *Hum. Brain. Mapp.*, vol. 28, no. 11, pp. 1178–1193, Nov. 2007.

[22] M. Fraschini, M. Demuru, A. Crobe, F. Marrosu, C. J. Stam, and A. Hillebrand, "The effect of epoch length on estimated EEG functional connectivity and brain network organisation," *J. Neural Eng.*, vol. 13, no. 3, Jun. 2016, Art. no. 036015.

[23] C. J. Stam, W. Hann, A. Daffertshofer, B. F. Jones, I. Manshanden, and A. M. C. Walsum, "Graph theoretical analysis of magnetoencephalographic functional connectivity in Alzheimer's disease," *Brain*, vol. 132, no. 1, pp. 213–224, Nov. 2009.

[24] G. Fraga González *et al.*, "EEG resting state functional connectivity in adult dyslexics using phase lag index and graph analysis," *Frontiers Hum. Neurosci.*, vol. 12, pp. 1–12, Aug. 2018.

[25] M. Hardmeier, F. Hatz, H. Bousleiman, C. Schindler, C. J. Stam, and P. Fuhr, "Reproducibility of functional connectivity and graph measures based on the phase lag index (PLI) and weighted phase lag index (wPLI) derived from high resolution EEG," *PLoS ONE*, vol. 9, no. 10, Oct. 2014, Art. no. e108648.

[26] H. Yu, X. Wu, L. Cai, B. Deng, and J. Wang, "Modulation of spectral power and functional connectivity in human brain by acupuncture stimulation," *IEEE Trans. Neural Syst. Rehabil. Eng.*, vol. 26, no. 5, pp. 977–986, May 2018.

[27] U. Zuchowicz, A. Wozniak-Kwasniewska, D. Szekely, E. Olejarczyk, and O. David, "EEG phase synchronization in persons with depression subjected to transcranial magnetic stimulation," *Frontiers Neurosci.*, vol. 12, pp. 1–17, Jan. 2019.

[28] X. Li, R. La, Y. Wang, B. Hu, and X. Zhang, "A deep learning approach for mild depression recognition based on functional connectivity using electroencephalography," *Frontiers Neurosci.*, vol. 14, pp. 1–20, Apr. 2020.

[29] W. Liu *et al.*, "Functional connectivity of major depression disorder using ongoing EEG during music perception," *Clin. Neurophysiol.*, vol. 131, no. 10, pp. 2413–2422, Oct. 2020.

[30] Z. Zhang *et al.*, "Frequency-specific functional connectivity density as an effective biomarker for adolescent generalized anxiety disorder," *Frontiers Hum. Neurosci.*, vol. 11, pp. 1–14, Dec. 2017.

[31] Z. Bian, Q. Li, L. Wang, C. Lu, S. Yin, and X. Li, "Relative power and coherence of EEG series are related to amnestic mild cognitive impairment in diabetes," *Frontiers Aging Neurosci.*, vol. 6, pp. 1–9, 2014.

[32] H. Yu, J. Liu, L. Cai, J. Wang, Y. Cao, and C. Hao, "Functional brain networks in healthy subjects under acupuncture stimulation: An EEG study based on nonlinear synchronization likelihood analysis," *Phys. A, Stat. Mech. Appl.*, vol. 468, pp. 566–577, Feb. 2017.

[33] J. X. Yang, H. J. Zhang, J. Ni, C. K. W. De Dreu, and Y. Ma, "Within-group synchronization in the prefrontal cortex associates with intergroup conflict," *Nature Neurosci.*, vol. 23, no. 6, pp. 754–760, Apr. 2020.

[34] S. Khare, V. Bajaj, S. Siuly, and G. R. Sinha, "Classification of schizophrenia patients through empirical wavelet transformation using electroencephalogram signals," in *Modelling and Analysis of Active Biopotential Signals in Healthcare*. Bristol, U.K.: IOP Science, 2020, pp. 1–26.

[35] K. Kroenke, R. L. Spitzer, and J. Williams, "The PHQ-9: Validity of a brief depression severity measure," *J. Gen. Internal Med.*, vol. 16, no. 9, pp. 606–613, Sep. 2001.

[36] R. L. Spitzer, K. Kroenke, J. B. Williams, and B. Löwe, "A brief measure for assessing generalized anxiety disorder: The GAD-7," *Arch. internal Med.*, vol. 166, no. 10, pp. 1092–1097, May 2006.

[37] H. Cai *et al.*, "A pervasive approach to EEG-based depression detection," *Complexity*, vol. 2018, Feb. 2018, Art. no. 5238028.

[38] D. J. Buysse, C. F. Reynolds, T. H. Monk, S. R. Berman, and D. J. Kupfer, "The Pittsburgh sleep quality index: A new instrument for psychiatric practice and research," *Psychiatry Res.*, vol. 28, no. 2, pp. 193–213, May 1989.

[39] H. Cai *et al. MODMA Dataset: A Multi-Modal Open Dataset for Mental-Disorder Analysis*. [Online]. Available: http://modma.lzu.edu.cn/data/index/

[40] X. Li, B. Hu, T. Xu, J. Shen, and M. Ratcliffe, "A study on EEG-based brain electrical source of mild depressed subjects," *Comput. Methods Programs Biomed.*, vol. 120, no. 3, pp. 135–141, Jul. 2015.

[41] B. T. Zhang, T. Lei, H. Liu, and H. S. Cai, "EEG-based automatic sleep staging using ontology and weighting feature analysis," *Comput. Math. Methods Med.*, vol. 2018, Sep. 2018, Art. no. 6534041.

[42] H. Peng *et al.*, "Removal of ocular artifacts in EEG—An improved approach combining DWT and ANC for portable applications," *IEEE J. Biomed. Health Inform.*, vol. 17, no. 3, pp. 600–607, May 2013.

[43] B.-T. Zhang, X.-P. Wang, Y. Shen, and T. Lei, "Dual-modal physiological feature fusion-based sleep recognition using CFS and RF algorithm," *Int. J. Autom. Comput.*, vol. 16, no. 3, pp. 286–296, Mar. 2019.

[44] R. Afshar, F. M. Mueller, and J. C. Shaffer, "Hilbert transformation of densities of states using Hermite functions," *J. Comput. Phys.*, vol. 11, no. 2, pp. 190–209, Feb. 1973.

[45] H. F. Si *et al.*, "Research on brain functional network and lie detection based on phase lag index," *Acta Electr. Sinica*, vol. 46, no. 7, pp. 1742–1747, Jul. 2018.

[46] X. Li, Z. Jing, B. Hu, J. Zhu, N. Zhong, M. Li, Z. J. Ding, J. Yang, L. Zhang, L. Feng, and D. Majoe, "A resting-state brain functional network study in MDD based on minimum spanning tree analysis and the hierarchical clustering," *Complexity*, vol. 2017, Jul. 2017, Art. no. 9514369.

[47] X. Liang, J. Wang, and Y. He, "Human connectome: Structural and functional brain networks," *Chin. Sci. Bull.*, vol. 55, no. 16, pp. 1565–1583, Jun. 2010.

[48] T. J. Whitford, C. J. Rennie, S. M. Grieve, C. R. Clark, E. Gordon, and L. M. Williams, "Brain maturation in adolescence: Concurrent changes in neuroanatomy and neurophysiology," *Hum. Brain Mapping*, vol. 28, no. 3, pp. 228–237, Mar. 2007.

[49] B. Zhang and P. Cao, "Classification of high dimensional biomedical data based on feature selection using redundant removal," *PLoS ONE*, vol. 14, no. 4, Apr. 2019, Art. no. e0214406.

[50] A. A. Fingelkurts, A. A. Fingelkurts, H. Rytsälä, K. Suominen, E. Isometsä, and S. Kähkönen, "Impaired functional connectivity at EEG alpha and theta frequency bands in major depression," *Hum. Brain Mapping*, vol. 28, no. 3, pp. 247–261, Mar. 2007.

[51] A. F. Leuchter, I. A. Cook, A. M. Hunter, C. Cai, and S. Horvath, "Resting-state quantitative electroencephalography reveals increased neurophysiologic connectivity in depression," *PLoS ONE*, vol. 7, no. 2, Feb. 2012, Art. no. e32508.

[52] C. Tas, M. Cebi, O. Tan, G. Hizli-Sayar, N. Tarhan, and E. C. Brown, "EEG power, cordance and coherence differences between unipolar and bipolar depression," *J. Affect. Disorders*, vol. 172, pp. 184–190, Feb. 2015.

[53] A. S. Dharmadhikari, A. L. Tandle, S. V. Jaiswal, V. A. Sawant, V. N. Vahia, and N. Jog, "Frontal theta asymmetry as a biomarker of depression," *East Asian Arch. Psychiatry*, vol. 28, no. 1, pp. 17–22, Mar. 2018.

[54] X. M. Ma *et al.*, "Research about alpha EEG asymmetry and self-consciousness in depression," *Brain Informatics and Health*, vol. 9919. Sep. 2016, pp. 94–103.

[55] M. D. Greicius *et al.*, "Resting-state functional connectivity in major depression: Abnormally increased contributions from subgenual cingulate cortex and thalamus," *Biol. Psychiatry*, vol. 62, no. 5, pp. 429–437, Oct. 2007.

[56] Y. Zhou *et al.*, "Increased neural resources recruitment in the intrinsic organization in major depression," *J. Affect. Disorders*, vol. 121, no. 3, pp. 220–230, Mar. 2010.

[57] C. G. Connolly *et al.*, "Resting-state functional connectivity of subgenual anterior cingulate cortex in depressed adolescents," *Biol. Psychiatry*, vol. 74, no. 12, pp. 898–907, Dec. 2013.

[58] J. Joormann and I. H. Gotlib, "Emotion regulation in depression: Relation to cognitive inhibition," *Cognition Emotion*, vol. 24, no. 2, pp. 281–298, Feb. 2010.

[59] S. J. J. Leistedt, N. Coumans, M. Dumont, J.-P. Lanquart, C. J. Stam, and P. Linkowski, "Altered sleep brain functional connectivity in acutely depressed patients," *Hum. Brain Mapping*, vol. 30, no. 7, pp. 2207–2219, Jul. 2009.

[60] S. Sun *et al.*, "Graph theory analysis of functional connectivity in major depression disorder with high-density resting state EEG data," *IEEE Trans. Neural Syst. Rehabil. Eng.*, vol. 27, no. 3, pp. 429–439, Mar. 2019.

[61] N. Masuda and K. Aihara, "Global and local synchrony of coupled neurons in small-world networks," *Biol. Cybern.*, vol. 90, no. 4, pp. 302–309, Apr. 2004.

[62] L. Cammoun *et al.*, "Connectome alterations in schizophrenia," *NeuroImage*, vol. 47, p. S157, Jul. 2009.

[63] Y. Li, D. Cao, L. Wei, Y. Tang, and J. Wang, "Abnormal functional connectivity of EEG gamma band in patients with depression during emotional face processing," *Clin. Neurophysiol.*, vol. 126, no. 11, pp. 2078–2089, Nov. 2015.

[64] M. Zhang *et al.*, "Randomized EEG functional brain networks in major depressive disorders with greater resilience and lower rich-club coefficient," *Clin. Neurophysiol.*, vol. 129, no. 4, pp. 743–758, Apr. 2018.

[65] J. Zhang *et al.*, "Disrupted brain connectivity networks in drug-naive, first-episode major depressive disorder," *Biol. Psychiatry*, vol. 70, no. 4, pp. 334–342, Aug. 2011.